

Realization of parametric resonances in a nanowire mechanical system with nanomanipulation inside a scanning electron microscope

Min-Feng Yu,^{1,*} Gregory J. Wagner,^{2,†} Rodney S. Ruoff,² and Mark J. Dyer¹

¹Zyvx Corporation, Advanced Technologies Group, 1321 North Plano Road, Richardson, Texas 75081

²Northwestern University, Department of Mechanical Engineering, 2145 Sheridan Road, Evanston, Illinois 60208

(Received 3 April 2002; published 2 August 2002)

We realize parametric resonances in a nanowire mechanical system using an oscillating electric field. Resonances at drive frequencies near $2f_0/n$, where f_0 is the nanowire's fundamental resonance frequency, for n from 1 to 4 were observed inside a scanning electron microscope, and analyzed. Such resonances were found to originate from the amplitude-dependent electric field force acting on the nanowire and can be described by the Mathieu equation, which has known regions of instability in the parameter space.

DOI: 10.1103/PhysRevB.66.073406

PACS number(s): 62.25.+g, 62.40.+i

Nanostructures such as nanotubes, nanorods, nanowhiskers, and nanoplatelets have attracted great attention recently due to the promise of applications in sensing, materials reinforcement, vacuum microelectronics, and microelectromechanical (MEMS) or nanoelectromechanical systems (NEMS). The extremely small physical dimensions of nanostructures imply high sensitivity to external perturbation, and this characteristic has been recently investigated for femto-gram mass measurement, and biomolecule and gas sensing.^{1,2} Physics similar to the type reported here may ultimately confer superior performance for future NEMS systems having nanostructure components.^{3,4}

Parametric resonance describes the resonance due to a parametric excitation (a periodically varying coefficient) in the homogeneous equation of motion of the system.⁵ In a single-degree-of-freedom mechanical system, parametric resonance described by the Mathieu equation is

$$\frac{d^2Y}{dt^2} + \mu \frac{dY}{dt} + (a + 2\varepsilon \cos \omega t)Y = 0, \quad (1)$$

where Y is an angular or displacement variable, μ is the damping constant, and a and ε are system parameters. For an undamped system ($\mu=0$), the theory predicts instabilities at $a=n^2/4$ for $n=1,2,\dots$, and regions of instability in the parameter space described by a and ε . Such instabilities result in parametric resonances of the system at drive frequencies of $2\omega_0/n$, where ω_0 is the natural resonance frequency of the system. This principle has been applied in optics or optoelectronics,⁶ in high sensitivity electronics,⁷ in superconducting Josephson junction devices,⁸ in electron Penning trapping,⁹ as well as in mechanical system analysis.⁵ The realization of high order parametric mechanical resonance in macroscopic systems is generally difficult due to mechanical energy losses and strict conditions applied at higher n determined by the system parameters; high order (for n up to 4) parametric mechanical resonance was only recently observed in microscale MEMS resonators.⁴

We report the discovery of up to four parametric resonances for cantilevered nanowires. A theory for a forced vibration system that includes a forcing term proportional to the amplitude of the resonance was used for the analysis, regions of instability were mapped, and hysteresis in the

parametric resonance response curve was observed. Excellent agreement between the theory and experiment was found.

Figure 1(a) shows the schematic of the experiment for the study of the resonance mechanics of nanowires. A dc bias and an ac signal from a sine wave signal generator, which generates the oscillating electric field, are applied between the nanowire and a counter electrode. By tuning the frequency of the ac signal, the cantilevered nanowire can be excited such that maximum amplitude is achieved when the frequency of the drive signal matches the mechanical resonance frequency of the nanowire. Such a technique has recently been demonstrated¹ to drive vibrations and to deduce the Young's modulus values of carbon nanotubes inside a transmission electron microscope. However, in the previous study,¹ the oscillating force applied on cantilevered nanotubes due to the interaction between the induced charge and the oscillating electric field was treated as a perturbation, and only the natural resonances were observed.

A nanomanipulation stage was developed for use inside a field emission scanning electron microscope (Leo1530 SEM).¹⁰ This stage is capable of nanometer resolution motion, and free-space manipulation and characterization of nanostructures by the probes controlled by the nanomanipulator.

A computerized data acquisition system for acquiring the amplitude versus frequency response curve was also developed. In the acquisition, the SEM beam control is first set in line scan mode¹¹ across the nanowire. The sine wave signal generator (Wavetek 2500) is programmed to tune the drive frequency at fixed step (10 Hz to 10 kHz depending on the frequency resolution needed for the response curve), and at each step, the SEM line scan signal is acquired and processed to obtain the amplitude of the driven nanowire at that driving frequency. Figure 1(b) shows an SEM image of a cantilevered boron nanowire¹² fixed at one end in a raw sample and an etched tungsten probe positioned near the free end of the nanowire as the electrode. The amplitude-drive frequency curve acquired at 10 Hz scan step [Fig. 1(c)] shows the typical Lorentzian shape for a fundamental mode resonance centered at $f_0=1.19832$ MHz; according to the full-width-at-half-height the quality factor Q is 2900 for this nanowire resonator (the Young's modulus of the nanowire is estimated to be 160 GPa). Alternatively, by setting the beam control for the SEM in "spot mode" so that the beam scan is stopped, a periodic signal from the SEM detector output can

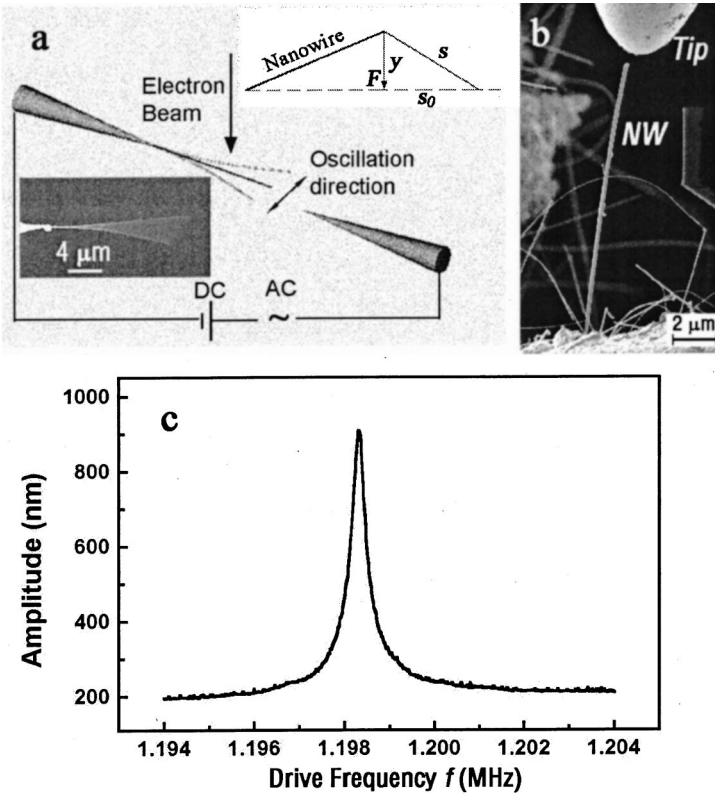


FIG. 1. (a) Schematic of the experimental setup inside the SEM showing the resonating boron nanowire under the applied dc bias and ac drive signal. The top-right hand inset in (a) shows the geometric relation between the nanowire and the drive electrode along the plane of the nanowire vibration, the bottom-left hand inset shows a representative boron nanowire in resonance. (b) SEM image showing a 12.6- μm long and 170-nm diameter boron nanowire fixed at one end in the raw sample and a closely positioned probe electrode tip. (c) The response curve for the mechanical resonance of the nanowire at its fundamental mode acquired at $V_{\text{dc}} = 0$ V and $V_{\text{ac}} = 300$ mV.

be acquired when the laterally resonating nanowire traverses the stationary electron beam. This technique provides a direct measurement of the real oscillating frequency and potentially phase of the nanowire.

The electric field-induced resonance of a cantilevered nanowire can be described as a nonlinear system with forced vibration. With a dc voltage V_{dc} and an ac drive signal $V_{\text{ac}} \cos(\Omega t)$, the forcing term $F(x, t)$ (where x is the distance along the nanowire) is $F(x, t) = -Q(x, t)V_{\text{dc}}^2(1 + \beta^2/2 + 2\beta \cos \Omega t + \beta^2/2 \cos 2\Omega t)$, where $\beta = V_{\text{ac}}/V_{\text{dc}}$, the angular drive frequency Ω is related to f through $\Omega = 2\pi f$, and $Q(x, t)$ is a function that depends on the geometry and electrical parameters of the system. For small displacements of the nanowire, $Q(x, t)$ can be approximated by an expansion in $y(x, t)$ (the displacement of the nanowire): $Q(x, t) = Q_0(x) + Q_1(x)y(x, t) + O(y^2)$. The electric field force on a segment of the wire is a Coulomb force.¹³

We include the effect of the electric field force to first order in y , and the equation of motion for the vibrating beam is

$$\rho A \frac{\partial^2 y}{\partial t^2} + c \frac{\partial y}{\partial t} + EI \frac{\partial^4 y}{\partial x^4} = -V_{\text{dc}}^2(1 + 2\beta \cos \Omega t)Q_1(x)y, \quad (2)$$

where ρ is the volume density (2460 Kg m⁻³ for boron), A is the cross sectional area, c is the damping coefficient, E is the bending modulus, and I is the area moment of inertia of the nanowire having a length L .

Integrating over the length L of the beam to remove the x dependence¹⁴ in Eq. (2) gives an equation for the time dependence of each natural resonance mode

$$\ddot{u}_i + \frac{c}{\rho A \Omega} \dot{u}_i + \frac{1}{\Omega^2} \left(\omega_i^2 + \frac{q_i V_{\text{dc}}^2}{\rho A \gamma_i} + \frac{2\beta q_i V_{\text{dc}}^2}{\rho A \gamma_i} \cos t \right) u_i = 0, \quad (3)$$

where $\omega_i = \kappa_i^2 \sqrt{EI/\rho A}$, $\gamma_i = L^{-1} \int_0^L \phi_i dx$ (note that ω_i is the natural angular frequency of mode i). Equation (3) has been made nondimensional by scaling time with Ω^{-1} and length with L . This equation has the form of the damped Mathieu equation [as described in Eq. (1)], with parameters $\mu = c/\rho A \Omega$, $a = \Omega^{-2}[\omega_i^2 + q_i V_{\text{dc}}^2/(\rho A \gamma_i)]$, $\varepsilon = \Omega^{-2} \beta q_i V_{\text{dc}}^2/(\rho A \gamma_i)$. The vibration in our experiments is the fundamental mode ($i=0$) resonance, for which $\kappa_0 \approx 1.875/L$ and $\gamma_0 \approx 0.783$. Since the Mathieu equation has points of instability at values of a given by $n^2/4$, according to Eq. (3) this occurs for values of the driving frequency given by $\Omega_R = (2/n) \sqrt{\omega_0^2 + q_0 V_{\text{dc}}^2/(\rho A \gamma_0)}$. Note that these resonances are not exactly proportional to the natural frequency ω_0 , but instead are shifted by a small amount dependent upon q_0 and V_{dc} . This deviation has not been included in previous studies,¹ but has been observed recently by Gao *et al.* in their study on the resonance of multiwalled carbon nanotubes¹⁵ (though in their qualitative analysis the dependence of the resonance frequency on the applied V_{dc} is considered to be the result of the increasing mechanical tension along the nanotube under increasing dc bias). There is also the possibility that permanent surface charge may be present in the system, which can contribute to the tension effect and thus the frequency shift.

We now present the experimental results on the parametric resonances of individual boron nanowires. Figure 2 shows the acquired amplitude-drive frequency curves of

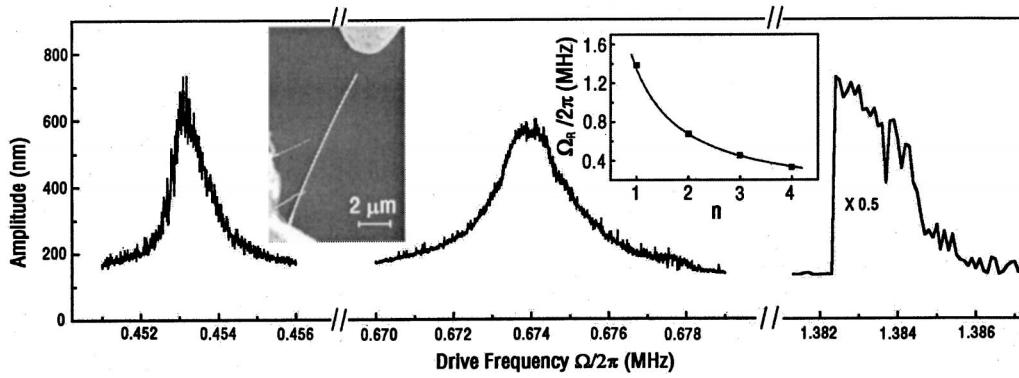


FIG. 2. The amplitude versus drive frequency curves for the parametric resonances f at 0.453 MHz (acquired at $V_{dc}=35$ V and $V_{ac}=1000$ mV), 0.674 MHz (acquired at $V_{dc}=0$ V and $V_{ac}=300$ mV) and 1.386 MHz (acquired at $V_{dc}=10$ V and $V_{ac}=300$ mV). The left hand inset shows the SEM image of the nanowire (11.6- μm long and 67-nm in diameter) and the probe electrode tip (placed 1.5 μm away from the free end of the nanowire). The right-hand inset shows the comparison between the drive resonance frequency (square) for the parametric resonances from the experiment and the curve according to the theory.

three parametric resonances centered at drive frequencies f of 0.453 MHz (close to $2f_0/3$), 0.674 MHz (the resonance frequency of the fundamental mode f_0), and 1.386 (close to $2f_0$) for a boron nanowire (the Young's modulus of the nanowire was estimated to be 230 GPa) as shown in the left hand inset in Fig. 2. The resonance at $f=0.329$ MHz (close to $f_0/2$) excited manually with $V_{dc}=0$ V and $V_{ac}=1$ V using another signal generator was also visually observed but the response curve was not acquired because the frequency was out of the range of the computer-controlled signal generator (0.4 MHz–1.1 GHz). A comparison between the experimental data (represented by solid squares in the plot) and the curve according to $\Omega_R=2\omega_0/n$ is plotted in the right-hand inset in Fig. 2, and shows an excellent agreement. The SEM spot mode method described above was used and it was found that the nanowire oscillated constantly near its fundamental frequency f_0 with the above four different drive frequencies, which is a characteristic of a parametric resonance system.

Regions of mechanical instability in parameter space are expected as a result of the Mathieu equation. Figure 3(a) shows such a stability chart for a nanowire having a length of 10 μm and a diameter of 114 nm for its parametric resonance $n=1$. The plot was obtained by acquiring 42 amplitude versus frequency response curves at 42 pairs of V_{dc} and V_{ac} voltages. From each acquired response curve, two threshold frequencies, one at the jump up point such as the point A and another at the smoothly rising up part of the curve such as the point B in the response curve as shown in Fig. 3(b), were determined. The jump down event such as at the point C in Fig. 3(b) depends on other high order perturbations in a large amplitude oscillation system, and is not related to the region of instability defined by the parametric resonance equation. The V_{dc} , V_{ac} , and threshold frequencies were then converted to a and ε according to formulas given above, which resulted in the upper and lower boundaries for the instability region as shown in Fig. 3(a). The plot clearly shows a “tongue” shape for the unstable region confined between the two linear boundaries as predicted by the Mathieu equation. The dashed lines in Fig. 3(a) are the predicted boundaries from the

theory for comparison. Mapping the stability chart for higher-order parametric resonance, such as for $n=3$, is difficult due to the higher excitation voltages needed for such mapping. Applying higher ac and dc voltage significantly disturbs the electron beam in the SEM imaging and thus the data acquisition.

Hysteresis is seen from the frequency response curve for the parametric resonance $n=1$ of the nanowire at constant dc and ac bias as shown in the inset in Fig. 3(b). Two curves

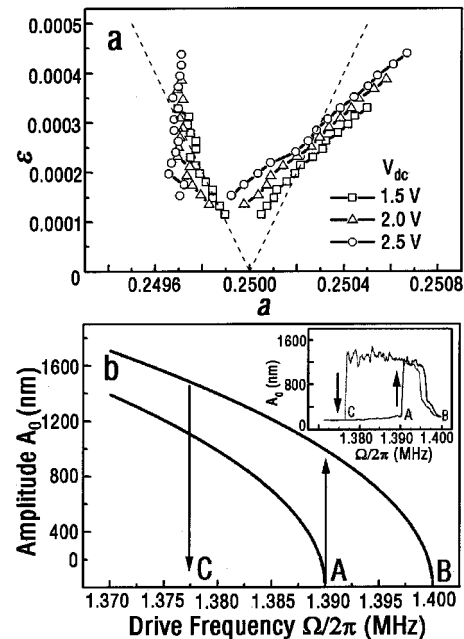


FIG. 3. (a) Stability diagram for the parametric resonance $n=1$ of a boron nanowire having a diameter of 114 nm and a length of 10 μm . The dashed lines indicate the boundaries according to the theory. (b) Amplitude-frequency response curve obtained from modeling for the parametric resonance $n=1$ described in Fig. 2. The arrowed lines indicate the locations of the possible jumps. The inset in (b) is the experimental result showing the hysteresis for the nanowire described in Fig. 2. The bias conditions for the experiment were $V_{dc}=17.6$ V and $V_{ac}=550$ mV.

acquired from a forward frequency sweep and from a backward frequency sweep are displayed. “Jump up” at point *A* and “jump down” at point *C* between the upper and lower branches of the response curve are clearly resolved, indicating that there is an unstable portion of the response curve between points *A* and *C* that is unattainable.

This hysteresis can be understood by considering the nonlinear force-deflection behavior of the nanowire. In parametric resonance, unlike resonance of a simple mass-stiffness system, finite damping alone is not sufficient to keep the amplitude from growing to infinity as time increases; rather, the nonlinear behavior of the system must provide the upper limit to amplitude growth. To demonstrate this, we consider an undamped version of the Mathieu equation $d^2u/dt^2 + (a + 2\varepsilon \cos t)u - \varepsilon\alpha u^3 = 0$, where α is assumed to give the relative size of a cubic nonlinearity in the system. Using a multitime expansion¹⁶ in the small parameter ε , and considering values of the parameter a near $\frac{1}{4}$ (so that $a = \frac{1}{4} + \varepsilon a_1$), we derive periodic solutions having the form $u = A_0 \cos(t/2 + \theta)$. Three solutions for the steady-state amplitude exist $A_0 = 0$, $A_0 = (2/\sqrt{3\alpha})(a_1 \pm 1)^{1/2}$. The presence of multiple stable solutions for $a_1 > -1$ explains the hysteresis seen in the experiment near $a = \frac{1}{4}$. Figure 3(b) shows the response curve obtained according to these solutions obtained from this model.

A parametrically driven cantilevered nanowire can be designed to operate near the boundary conditions according to the stability chart, and could provide very effective response to either individual molecule or nanoparticle attachment by threshold transition for making “supersensitive” sensors of, e.g., molecular adsorbates. A parametric resonator has also a unique feature that a normal resonator does not have. Parametric resonances only occur when the parameters lie in a *particular range*. For the case reported in this paper, three adjustable parameters define the stability chart: the ac and dc voltage and the frequency of the oscillating electric field. Thus, an array of nanoresonators can be envisioned where resonance is literally “turned on” from the nonresonance condition, or vice versa, by the adsorption of single molecules, and the resonance condition can be readily tuned by simple adjustments of these parameters. Further investigation and development of such high selectivity and high sensitivity sensors are suggested.

We thank W. E. Buhro and RSR for supplying the B nanowires; the synthesis of these B nanowires was supported by the Semiconductor Research Corporation (98-MJ-651). G.J.W. and R.S.R. appreciate support from the Office of Naval Research Miniaturized Intelligent Sensor (MIS) program, and R.S.R., support from the NSF. We thank J. Lee, W.-K. Liu, P. Pehrsson, T. Kowalewski, and W. E. Buhro for valuable comments.

*Email address: mfyu@uiuc.edu

†Email address: g-wagner@northwestern.edu

¹P. Poncharal, Z. L. Wang, D. Ugarte, and W. A. de Heer, *Science* **283**, 1513 (1999).

²J. Kong, N. R. Franklin, C. Zhou, M. G. Chapline, S. Peng, K. Cho, and H. Daitl, *Science* **287**, 622 (2000); T. W. Tomblor, C. Zhou, L. Alexseyev, J. Kong, H. Dai, C. S. Jayanthi, M. Tang, and S.-Y. Wu, *Nature (London)* **405**, 769 (2000); D. Srivastava, D. W. Brenner, J. D. Schall, K. D. Ausman, M.-F. Yu, and R. S. Ruoff, *J. Phys. Chem. B* **103**, 4330 (1999); Y. Cui, Q. Wei, H. Park, and C. M. Lieber, *Science* **293**, 1289 (2001); B. Ilic, D. Czaplewski, H. G. Craighead, P. Neuzil, C. Campagnolo, and C. Batt, *Appl. Phys. Lett.* **77**, 450 (2000).

³H. G. Craighead, *Science* **290**, 1532 (2000).

⁴K. L. Turner, S. A. Miller, P. G. Hartwell, N. C. MacDonald, S. H. Strogatz, and S. G. Adams, *Nature (London)* **396**, 149 (1998).

⁵A. H. Nayfeh and D. T. Mook, *Nonlinear Oscillations* (Wiley, New York, 1979).

⁶E. Rosencher, A. Fiore, B. Vinter, V. Berger, P. Bois, and J. Nagle, *Science* **271**, 168 (1996).

⁷K.-H. Löcherer and C.-D. Brandt, *Parametric Electronics: An Introduction* (Springer-Verlag, New York, 1982).

⁸K. F. Loe and E. Goto, *DC Flux Parametron: A New Approach to Josephson Junction Logic* (World Scientific, Philadelphia, 1986).

⁹C. H. Tseng, D. Enzer, G. Gabrielse, and F. L. Walls, *Phys. Rev. A* **59**, 2094 (1999).

¹⁰M.-F. Yu, M. J. Dyer, J. Chen, and K. Bray, in *IEEE-NANO 2001 International Conference, Maui, October 28-30, 2001* (to be

published).

¹¹The SEM line scan shows a narrow peak with a width roughly equal to the diameter of the nanowire when the nanowire is essentially stationary; it shows a broader plateau when the nanowire is driven into oscillation, and the width of the plateau corresponds to the amplitude envelope of the oscillation.

¹²C. J. Otten, O. R. Lourie, M.-F. Yu, J. M. Cowley, M. J. Dyer, R. S. Ruoff, and W. E. Buhro, *J. Am. Chem. Soc.* **124**, 4564 (2002).

¹³For example, for the geometry shown in the inset in Fig. 1(a) in the paper, where the counter electrode is placed in line with the nanowire axis, the forcing has the form $Q(x,t) \propto y/(s_0^2 + y^2)^{1/2} = y s_0^{-1} [1 - y^2/2s_0^2 + O(y^4)]$, where s_0 is the distance between the free end of the stationary nanowire and the end of the opposite probe. In this configuration $Q_0 = 0$. We will therefore consider only this case in the ensuing analysis; the analysis does not change greatly if $Q_0 \neq 0$.

¹⁴Both $y(x,t)$ and $Q_1(x)$ can be written in terms of a modal decomposition $y(x,t) = \sum_{i=0}^{\infty} u_i(t) \phi_i(x)$, $Q_1(x) = \sum_{i=0}^{\infty} q_i \phi_i(x)$, where the modes $\phi_i(x)$ are solutions of the equation $\phi_i'''' = \kappa_i^4 \phi_i$ with the appropriate spatial boundary conditions ($\phi_i = \phi_i' = 0$ at $x=0$, $\phi_i'' = \phi_i''' = 0$ at $x=L$ for the case of the singly clamped nanowire). The modes are scaled such that they form an orthonormal set $L^{-1} \int_0^L \phi_i \phi_j dx = \delta_{ij}$, where δ_{ij} is the Kronecker delta.

¹⁵R. Gao, Z. Pan, and Z. L. Wang, *Appl. Phys. Lett.* **78**, 1757 (2001).

¹⁶C. M. Bender and S. A. Orszag, *Advanced Mathematical Methods for Scientists and Engineers* (McGraw-Hill, New York, 1978).